

# PERFORMANCE TEST OF MASS-PRODUCTION HWR CRYOMODULES FOR SCL32\*

Youngkwon Kim<sup>†</sup>, Danhye Gil, Hyojae Jang, Hyunik Kim, Yong Woo Jo, Jaehee Shin, Jong Wan Choi, Moo Sang Kim, Min Ki Lee, Jongdae Joo, Hoechun Jung, Myeun Kwon, IBS, Daejeon, Korea  
 Younguk Sohn, PAL, Pohang, Korea

## Abstract

Mass production of the HWR (half wave resonator) cryomodules for SCL32 of RAON had been conducted since 2018 and all cryomodules were installed in the SCL3 tunnel in 2021. Total number of the HWR cavities and the HWR cryomodules are 106 and 34, respectively. Cryomodule performance test was started in September 2020 and finished in October 2021, except for one bunching cryomodule that will be installed in front of the high energy linac. The detailed procedure and the results of performance test is reported in detail.

## INTRODUCTION

The Rare isotope Accelerator Complex for ON-line Experiments (RAON) has been built for providing beam of exotic rare isotope of various energies at the Institute for Basic Science (IBS) [1-2]. The layout of RAON is shown in Figure 1. The low energy superconducting linac (SCL3) of RAON is composed of 22 quarter wave resonator (QWR) cryomodules and 35 half wave resonator (HWR) cryomodules including two bunching HWR cryomodules in a post-accelerator to driver linac (P2DT). The high-energy superconducting linac (SCL2) use two types of single spoke resonator (SSR1 and SSR2). 23 SSR1 cryomodule and 23 SSR2 cryomodule are required for SCL2. Total number of the QWR cavity is 22 and that of the HWR cavity is 106 since 15 HWR cryomodules are holds two cavities in them (HWR CMA) while 19 HWR cryomodules have four cavities in them (HWR CMB). The RF parameters of QWR

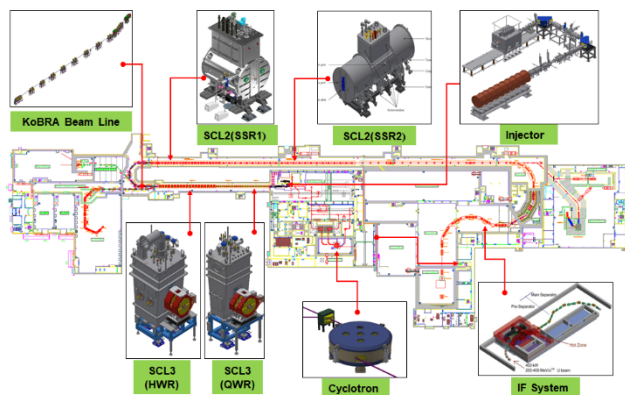


Figure 1: Layout of RAON

Table 1: RF Parameters of QWR and HWR Cavity

	QWR	HWR
$\beta_{opt}$	0.047	0.12
$f$ [MHz]	81.25	162.5
$L_{eff}$	173.5	221.5
$R/Q$ [ $\Omega$ ]	469	295
$E_p/E_{acc}$	5.7	5.2
$B_p/E_{acc}$ [mT/(MV/m) <sup>2</sup> ]	10.4	9
$E_{acc}$ [MV/m]	6.1	6.6
$V_{acc}$ [MV]	1.06	1.46
$QR_s$	18.1	36.8

and HWR cavities are listed in Table 1. Total number of SSR1 and SSR2 cavities are 69 and 138, respectively. The mass-production of QWR and HWR cryomodules were already finished and the prototyping of the cryomodules for SCL2 section are still on-going.

The mass-production of HWR cryomodules was started in May, 2018. Fabrication of the sub-components such as cavity, coupler, tuner and cryomodule was done by the domestic vendor and the surface treatment of the cavity and the assembly of cryomodule were done in both vendor site and own facility of IBS. The vertical test (VT) and the horizontal test (HT) had been done in two SRF test facilities of IBS. One is off-site test facility that has 2 VT pits, 2 HT bunkers, and 70 L/h helium liquefier and another is on-site test facility that has 3 VT pits, 3 HT bunkers, and 140 L/h helium liquefier. The cavities that had passed the vertical test were assembled in the cryomodules. Performance test of HWR cryomodules was started in September 2020 and finished in November 2021 except for one cryomodule that will be installed at the end of P2DT section. The low energy linac of RAON was installed in the tunnel on December 2021. SCL3 will be cooled down in September 2022 and the first beam injection to SCL3 is planned to be in October 2022[3].

## TEST SETUPS AND PROCEDURE

Performance test of cryomodules were conducted in the HT bunkers at both test facilities. Figure 2 shows the test setups in the bunker. Cryogenic fluid such as liquid nitrogen and liquid helium were supplied from the helium liquefier and LN2 tanks, respectively through the flexible insulated transfer lines. Two RF transmission lines were installed in the bunkers and connected with power couplers.

\* This work was supported by the Rare Isotope Science Project of Institute for Basic Science funded by Ministry of Science and ICT and NRF of Korea (2013M7A1A1075764)

<sup>†</sup> ykkim78@ibs.re.kr

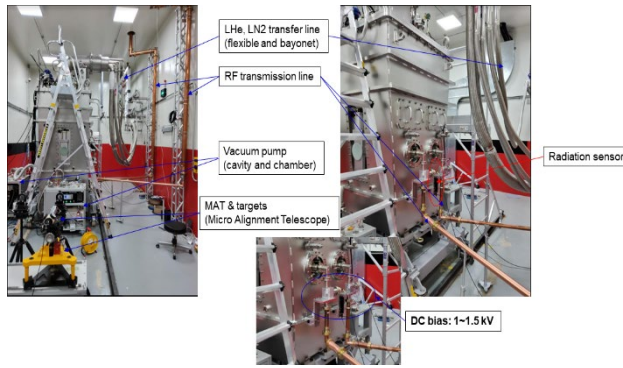


Figure 2: Test setups in the HT bunker for HWR cryomodules

The solid state power amplifiers (SSPA) were located outside the bunker. The DC biases were utilized to suppress the multipaction of the power couplers. 1.5 kV DC voltage was supplied to the DC bias during the experiments. Two vacuum pumps were used for evacuating cavity string and insulation vacuum. The vacuum pumping station for the cavity string had slow pump-down system that can control the initial pumping speed. The micro alignment telescope and reference targets were utilized to measure the displacement of the cavities. Radiation sensor was installed around the power coupler to monitor the X-ray due to the field emission of the cavities.

When the cryomodule arrived on the test facility from the vendor's assembly site which is approximately 140 km from the test facility, vacuum of cavities was checked just after the cryomodule was unloaded from the low-bed trailer. Then, the cryomodule was moved into the bunker and the routine installation and check procedure were conducted. Frequency of each cavity was measured and the

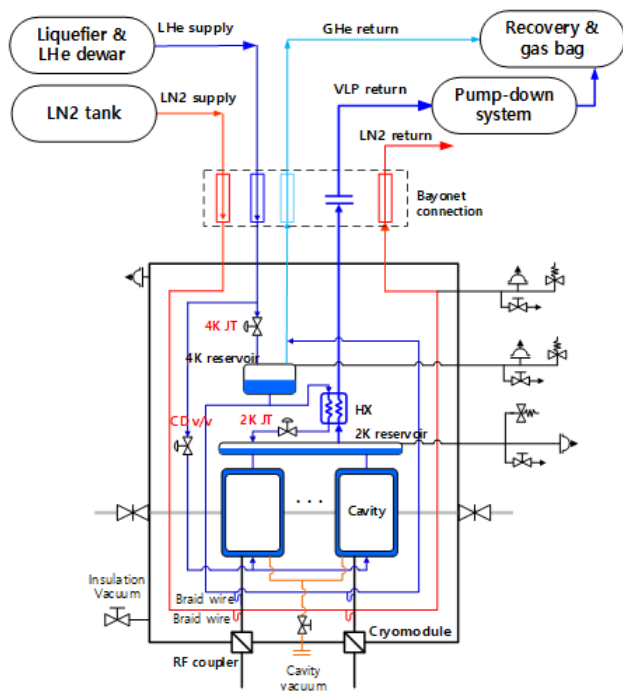


Figure 3: P&ID of cryomodule and cryogenic system for performance test

tuner operation test was conducted before evacuating the cryomodule. The displacement of each cavity was measured before and after the transportation, and it is also measured after the insulation vacuum pump-down and after the cavity cool-down.

When the room temperature work were finished, cool-down of cryomodule was started. P&ID of the cryomodule and the cryogenic system for the performance test can be found in Fig. 3. Cryomodule has two LHe reservoirs. One is called 4 K reservoir that stores 4.2 K liquid helium to supply single phase liquid helium to heat exchanger and to cool the 4 K thermal intercept of power coupler by a thermosiphon. Another one is 2 K reservoir that is installed on the top of the cavity string and stores superfluid helium at 2.05 K. Two cryogenic valves (4K JT and 2 K JT in Fig. 3) are utilized to control the helium mass flow rate for the reservoirs. One valve which is called cool-down valve (CD v/v in Fig. 3) is utilized only in the initial cool-down process. The cool-down was started with the supply of liquid nitrogen to thermal shield. Liquid nitrogen was utilized to cool the thermal shield for the test while 40 K gaseous helium will cool down the thermal shield in the tunnel. Liquid helium was supplied to the cryomodule approximately one day after the liquid nitrogen supply. Liquid helium was initially supplied to the bottom of the cavity string through the cool-down valves. When the liquid helium reached the 2 K reservoir, the cool-down valve was closed gradually and the 4 K JT valve was opened to store liquid helium in 4 K reservoir. When the liquid helium level in both reservoirs were observed the two JT valves were started to controlled automatically for maintaining liquid helium level about 50%. Then, the static thermal load was measured periodically during the experiment.

RF power was supplied to the cavity when the liquid helium level in the both reservoirs were maintained stably. The HWR cavity has multipacting band below 1.7 MV/m as shown in Fig. 4. It is known that the cavity in the multipacting band since the transmitted power ( $P_t$ ) rarely increases even though the forward power ( $P_f$ ) increases in stepwise. Therefore, the forward power supplied in early

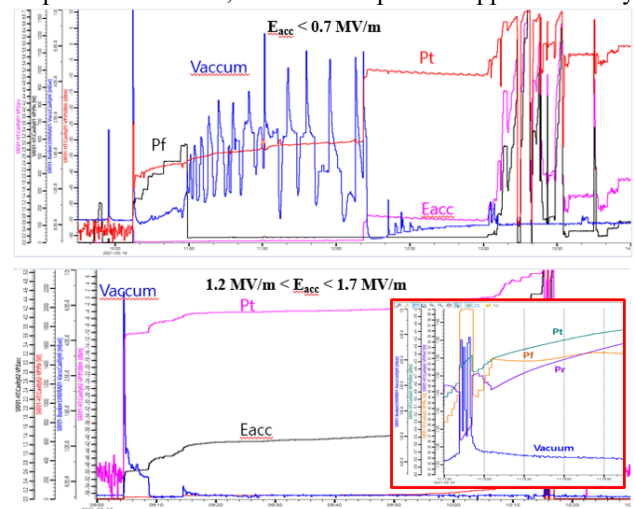


Figure 4: Multipacting conditioning procedure ( $P_f$ : forward power,  $P_t$ : transmitted power,  $P_r$ : reflected power)

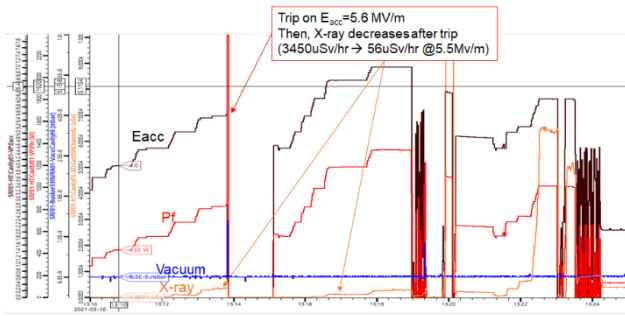


Figure 5: Conditioning effect during initial RF application stage of multipacting conditioning was 20 W. It is also shown that the cavity vacuum level fluctuated up to middle of  $10^{-8}$  mbar during the multipacting conditioning. There are two different aspect of multipacting for HWR cavity according to the field gradient of the cavity as shown in Fig. 4. In the second multipacting band which is the field gradient between 1.2 MV/m and 1.7 MV/m, the transmitted power seems to increase in the same manor when the forward power is supplied in stepwise. However, the reflected power ( $P_r$ ) decrease in stepwise and the transmitted power and the reflected power increase gradually when the forward power maintains the same value as shown in Figure 4. It means that there exists a loss due to the multipacting in the cavity and it is gradually conditioned.

After the multipacting conditioning was finished, forward power was increased gradually to excite the electric field of the cavity. It was observed that the radiation started to be generated at low field gradient during the initial RF application. It was easily conditioned after the quench or the breakdown of the cavity as shown in Figure 5. It is shown that X-ray level was dramatically decreased after the conditioning event. If the field emission was not properly conditioned when the field gradient reached above the operating gradient of the cavity, it was tried to be conditioned with pulsed RF power. The width of the pulse was generally 20 ms and repetition of it was adjusted according the thermal load of the cavity. The peak field gradient by the pulsed RF power was limited around 1.5 times larger than operating field gradient since the maximum power of SSPA is 4 kW. The X-ray level was carefully monitored during the pulse conditioning. It was easily recognized that the breakdown or the conditioning event occurred by the sudden drop or decrease of X-ray level. The dynamic thermal load of the cavity was measured before and after the pulse conditioning to monitor the performance change of the cavity.

The dynamic thermal load of the cavities in the cryomodule reached reasonably small at 4 K, the 2 K pump-down were started. It took approximately 30 minutes with warm-pumping system. The  $df/dp$  of the cavities were measured with around 3 MV/m of field gradient during the pump-down process. Loaded Q ( $Q_L$ ) and s-parameters were measured with a vector network analyzer to calibrate the external Q value of pickup ( $Q_i$ ) [4]. The  $Q_i$  value measured in the vertical test was utilized before the calibration process. The dynamic thermal load of each cavity was measured by the boil-off calorimetry. The dynamic thermal

**Technology**

**Cryomodules and cryogenics**

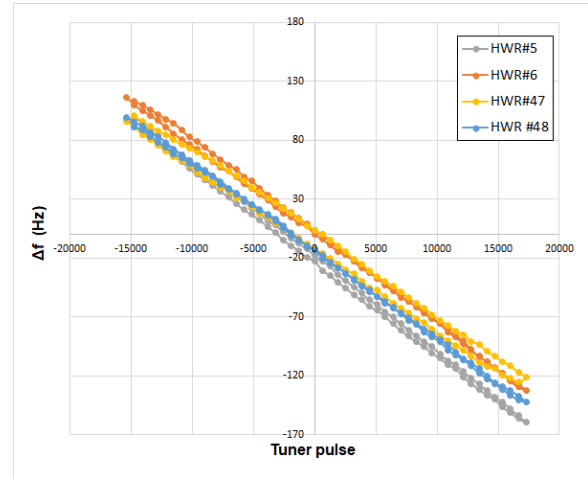


Figure 6: Narrow range tuner test results

loads was measured while each cavity was excited in operating field gradient and the static thermal load was also measured to know the dynamic thermal load of each cavity. Then, the tuner operation test and the LFD measurement were conducted. Tuner test was done in both wide ( $\pm 2$ kHz) and narrow ( $\pm 150$ Hz) frequency range. The typical results of the narrow range tuner test are shown in Figure 6. Most tuner showed linear response but some tuners had hysteresis such as the tuner of HWR #48 in the figure.

**TEST RESULTS**

The thermal load measurement results are shown in Figure 7. The total thermal load requirement for HWR CMA and HWR CMB are 14 W and 26 W at 2.05 K and 6.6 MV/m field gradient for every cavity, respectively. Every cryomodule satisfies the total thermal load requirement. The dynamic thermal load shown in the figure are the sum of the dynamic thermal loads of all cavities in the cryomodule. Average dynamic thermal load the HWR cavity is 3 W and  $Q_0$  is  $2.4 \times 10^9$ . It is noted that the static thermal loads in the figure were not measured at the thermal equilibrium of the cryomodules. It took more than one or two weeks for the cryomodules to reach their thermal equilibrium as

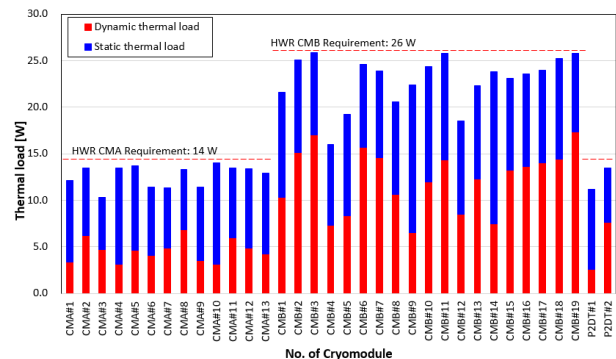


Figure 7: Thermal load measurement results for HWR cryomodules

Content from this work may be used under the terms of the CC BY 4.0 licence (© 2021). Any distribution of this work must maintain attribution to the author(s), title of the work, publisher, and DOI

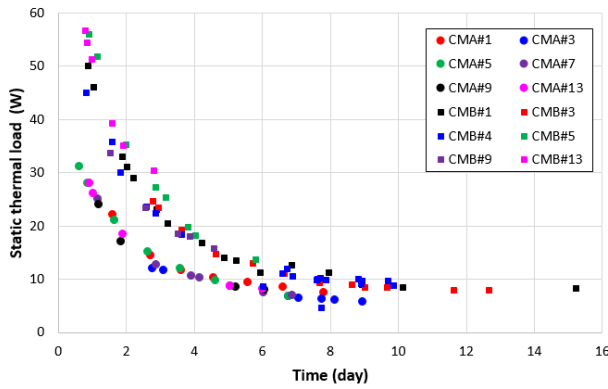


Figure 8: Tendency of static thermal load change

shown in Fig. 8. The performance tests were finished when the total thermal load met the requirements though the static thermal load did not reach its steady-state. The final static thermal load that we had measured were 5.6 W and 8.3 W for HWR CMA and HWR CMB, respectively while the average static thermal load measured during the experiments were 8.0 W and 10.7 W, respectively.

The mechanical properties such as  $df/dp$  and LFD of the HWR cavities were also measured and the results are shown in Fig. 9. The average values of  $df/dp$  and LFD in horizontal test are  $-7.2$  Hz/mbar and  $-3.2$  Hz/(MV/m)<sup>2</sup>, respectively. Also, some mechanical properties measured in vertical test were plotted in the same figure for the comparison. Since the tuner was not installed during the vertical test, it is known that the stiffness of the cavities increased by the tuner in the cryomodule. The  $df/dp$  and LFD values measured in the horizontal test reduced more than 45% compared with those measured in vertical test.

The external Q values were measured with a vector network analyzer and the results are plotted in Fig. 10. These values are very sensitive to the position of the inner conductor of the pickup and the power coupler. The length of the inner conductor of the pickup and the coupler were relatively easy to be controlled during the fabrication and the assembly. It seems that the distribution of the external Q values are mainly affected by the length of the pickup and the coupler ports. The pickup external Q ( $Q_t$ ) values are two orders higher than the average  $Q_0$  values of the cavities as expected. The operating bandwidth and the required RF power are affected by the coupler external Q ( $Q_c$ ) value. The average operating bandwidth is 140 Hz while the minimum is 90 Hz.

## CONCLUSION

The 15 HWR CMA and the 19 HWR CMB for low energy linac (SCL32) and bending section (P2DT) were successfully fabricated, tested and installed in the tunnel. The installed cryomodules were connected with the CDS (cryogenic distribution system) including the warm piping and

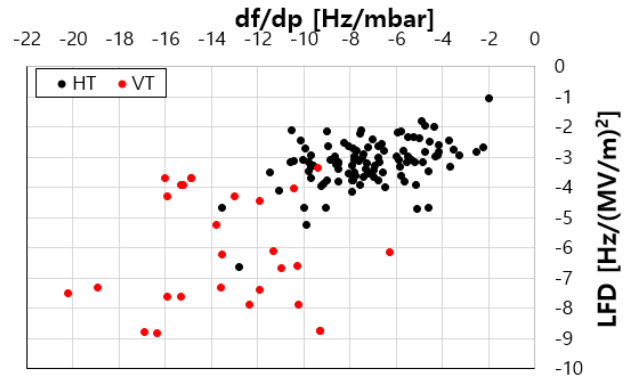


Figure 8:  $df/dp$  and LFD measurement results

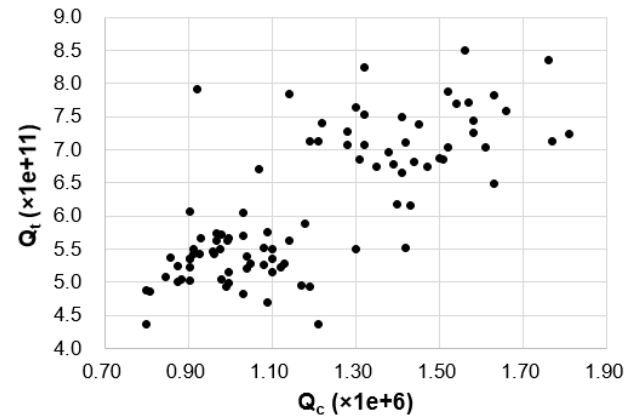


Figure 10:  $Q_t$  and  $Q_c$  measurement results

assembled with warm sections. The cryomodules are waiting for the cool-down and commissioning. The performances and the characteristics of 106 HWR cavities were also tested and measured individually after the cryomodule assembly.

The preparation and test procedure were well established and the personnel of RISP were properly trained during the mass production of SCL3 cryomodules. The lessons learned will be useful for the development and construction of the SCL2.

## REFERENCES

- [1] S. K. Kim, "Rare Isotope Science Project: Baseline Design Summary", Daejeon, Korea, IBS, 2012.
- [2] D. Jeon *et al.*, "Design of the RAON Accelerator Systems", *J. Korean Phys. Soc.*, vol. 65, no. 7, p. 1010, 2014. doi:10.3938/jkps.65.1010
- [3] H. J. Kim *et al.*, "Commissioning Status of the RAON Superconducting Accelerator", in *Proc. IPAC'22*, Bangkok, Thailand, Jun. 2022, pp. 2399-2401. doi:10.18429/JACoW-IPAC2022-THOXGD3
- [4] H. Hahn *et al.*, "Calibration of the ERL cavity FPC and PU couplers", 2010. doi:10.2172/1013467